SEISMIC BEHAVIOR OF REINFORCED CONCRETE MULTI-STORY BUILDINGS WITH CONFINED CONCRETE

Van Tu Nguyen[1,*], Xuan Dai Nguyen[1], Quoc Ky Le[1]

[1]*Le Quy Don Technical University*

Abstract

The paper presents the seismic analysis method of the reinforced concrete multi-story buildings employing Mander's nonlinear model for confined concrete behavior and bilinear model for reinforcement behavior. The action of earthquakes on the building is analyzed by using the time-history analysis method. The building structures are modeled by the finite element method based on the OpenSees software. The obtained responses of the internal forces, displacements, strain, and stress are highly consistent with the considered model suggesting that it is practically effective for the seismic-resistant design of the reinforced concrete buildings.

Keywords*: Confined concrete; unconfined concrete; stress-strain model of confined concrete; core concrete; nonlinear analysis of reinforced concrete frame; cover concrete.*

1. Introduction

In the practical design of reinforced concrete buildings, the material properties of structures are simplified as homogeneous materials with linear elastic behavior that is characterized by Young's modulus, stress, and strain of only concrete components [1, 2]. Consequently, the contributions of reinforcements are not often taken into account in the mechanical properties (stiffness). In this way, some finite element analysis softwares are commonly used such as Etabs, SAP2000 [3].

In the available concrete design codes [1, 2, 4], the standard compressive strength of concrete is generally measured by breaking cylindrical (or cube) concrete specimens at 28 days after casting in a compression-testing machine [1]. They are axial compression tests with lateral expansions. However, in reinforced concrete structures, there are always concrete parts limited by confinement reinforcement. Tests have shown that the confinement of concrete confined by suitable arrangements of transversal reinforcement results in a significant increase in both the strength and the ductility of compressed concrete [5]. The magnitude of these increases is established from various confinement parameters. However, it is not easy to explicitly characterize the mechanical behavior of confined concrete due to different parameter variables, such as the confinement type of rectilinear ties, the compressive strength of concrete, and the volumetric ratio and strength of rectilinear ties, etc. [6].

[*] Email: nguyentu@lqdtu.edu.vn
https://doi.org/10.56651/lqdtu.jst.v4.n02.344.sce

Many attempts have been conducted to describe the stress-strain relation of confined concrete. Sheikh et al. [7, 8], and Chung et al. [6] made analytical and experimental studies on the mechanism of confined concrete with various parameters. The authors introduced the concept of the effective confined concrete area and presented its stress-strain relationships. Based on the stress-strain relationship of unconfined concrete, Kent and Park [9] developed a specific model for confined concrete. Scott et al. [10] modified the model provided by Kent and Park. Mander et al. [5, 11] realized the confinement effects according to various configurations of lateral ties and presented a stress-strain relationship of confined concrete as shown in Figure 2a. Légeron and Paultre [12] proposed the new confinement model based on strain compatibility and the transverse force equilibrium to predict the effectiveness of transverse reinforcements. Paultre and Légeron [13] proposed new equations for the design of confinement reinforcements for ductile earthquake-resistant rectangular and circular columns based on the performance measured in terms of curvature demand.

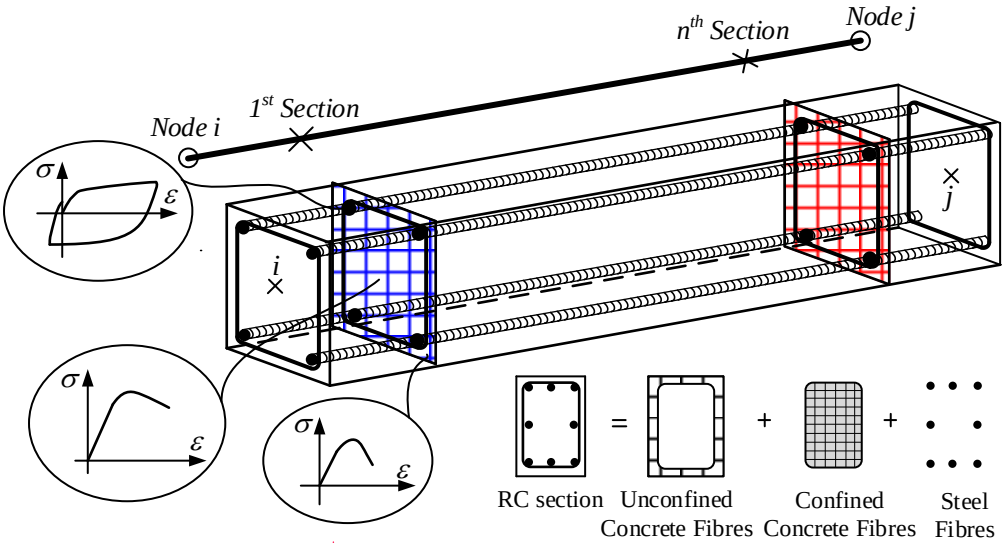

Figure 1. Fiber-reinforced concrete cross-section.

The nonlinear time-history analysis method has been widely used in the seismic analysis of reinforced concrete building structures. It essentially provides the complete nonlinear response history of structures subjected to earthquake ground motions. To study the nonlinear behavior of concrete and reinforcement, many authors have proposed the case study method such as Pinho [14], Clough [15], Cheng et al. [16] that have been integrated into commercial finite element software as SAP2000, Etabs [3]. However, the accuracy of these methods strongly depends on the time step, analysis methods, and mesh size, etc.

In the post-elastic analysis of concrete structure, the two typical models have been commonly used such as the concentrated plasticity model and the distributed plasticity model. The concentrated plasticity model is simple, but the material behavior is found less consistent with test results [17]. Consequently, it provides a low accuracy. The most common distributed plasticity model is the fiber model. In the fiber modeling, the sectional stress-strain state of the elements is obtained from the integration of the nonlinear uniaxial stress-strain response of individual fibers in which the section is subdivided, distinguishing steel, confined, and unconfined concrete, as illustrated in Figure 1. Based on this methodology, the Pacific Earthquake Engineering Research Center has developed the Open System for Earthquake Engineering Simulation (OpenSees) [18].

OpenSees has been known as open-source software for structural analysis based on the finite element method that can particularly simulate the structure subjected to earthquakes with various material behavior models and many analysis methods. Some typical studies have employed OpenSees to analyze the structure such as Melo et al. calculated the beam structures subjected to cyclic loading [19]; Tran Ngoc Cuong has integrated the CHHT2 method into OpenSees software to analyze a building of 10 floors with only beam and column structures and without slabs and walls [20].

This paper aims to study the seismic behavior of a reinforced concrete multi-story building by nonlinear time-history analysis method and using OpenSees open source. Mander's nonlinear model [5] is employed to model the confined concrete compressive behavior (i.e., without tension) and the bilinear model is used for reinforcement behavior, as shown in Figure 2b.

2. Formulations and method

2.1. Stress-strain model of confined concrete

Based on the stress-strain model of confined concrete of Mander et al. [5], for a slow (quasi-static) strain rate and monotonic loading, the longitudinal compressive concrete stress f_c is given by Eq. (1):

$$f_c = \frac{f'_{cc} xr}{r - 1 + x^r}, \tag{1}$$

where f'_{cc} is the compressive strength of confined concrete.

$$f'_{cc} = f'_{co}\left(-1.254 + 2.254\sqrt{1 + \frac{7.94 f'_l}{f'_{co}}} - 2\frac{f'_l}{f'_{co}}\right); \tag{2}$$

$$x = \frac{\varepsilon_c}{\varepsilon_{cc}}, \tag{3}$$

where f'_{c0} and f'_l are the unconfined concrete strength and effective lateral confining pressure, respectively; ε_c is the longitudinal compressive concrete strain.

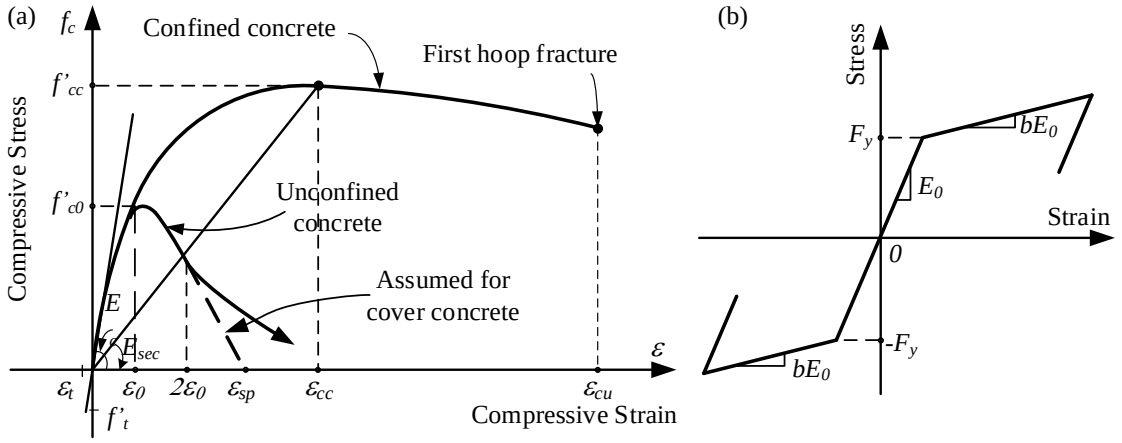

Figure 2. Stress-strain model of: (a) confined and unconfined concrete; (b) reinforcing bars.

Richart et al. (1928) suggested:

$$\varepsilon_{cc} = \varepsilon_{co}\left[1+5\left(\frac{f'_{cc}}{f'_{co}}-1\right)\right], \tag{4}$$

where f'_{c0} and ε_{c0} are the unconfined concrete strength and corresponding strain, respectively. Generally, $\varepsilon_{c0} = 0.002$ can be assumed.

$$r = \frac{E_c}{E_c - E_{\sec}}, \tag{5}$$

where E_c is the tangent modulus of elasticity of the concrete,

$$E_c = 5000\sqrt{f'_{co}} \text{ (MPa)}; \tag{6}$$

$$E_{\sec} = \frac{f'_{cc}}{\varepsilon_{cc}}. \tag{7}$$

To define the stress-strain behavior of the cover concrete (outside the confined core concrete area), the part of the falling branch in the region where $\varepsilon_c > 2\varepsilon_{c0}$ is assumed to be a straight line that reaches zero stress at the spalling strain, ε_{sp}.

2.2. Effect of confinement bars for confined concrete section

A specific approach, which is similar to the one used by Sheikh and Uzumeri (1980) [8], is adopted to determine the effective lateral confining pressure on the

concrete section. The maximum transversal pressure from the confining steel can only be effectively exerted on that part of the concrete core where the confining stress has fully developed due to arching action. Figure 3 shows the arching action that is assumed to occur between the levels of rectangular hoop reinforcement. Midway between the levels of the transversal reinforcement, the area of ineffectively confined concrete will be the largest and the area of effectively confined concrete core A_e will be the smallest.

When using the stress-strain relationship (Eq. (1)), for computing the strength and ductility of columns, it is conveniently assumed that the confined concrete area is considered the concrete part within the center lines of the perimeter spiral or hoop, A_{cc}. To allow for the fact that $A_e < A_{cc}$, it is considered that the effective lateral confining pressure is

$$f_l^{'} = f_l k_e, \tag{8}$$

where f_l is the lateral pressure from the transversal reinforcement, assumed to be uniformly distributed over the surface of the concrete core;

$$k_e = \frac{A_e}{A_{cc}}, \tag{9}$$

where k_e is the confinement effectiveness coefficient; A_e is the area of effectively confined concrete core;

$$A_{cc} = A_c\left(1-\rho_{cc}\right), \tag{10}$$

where ρ_{cc} is the ratio of area of longitudinal reinforcement to area of core of section; and A_c is the area of core of section enclosed by the center lines of the perimeter hoop.

In Figure 3, the arching action is again assumed to act in the form of second-degree parabolas with an initial tangent slope of 45°. Arching occurs vertically between layers of transversal hoop bars and horizontally between longitudinal bars. The effectively confined area of concrete at hoop level is found by subtracting the area of the parabolas containing the ineffectively confined concrete. For one parabola, the ineffectual area is $\left(w_i^{'}\right)^2$, where w_i' is the i^{th} clear distance between adjacent longitudinal bars (see Figure 3). Thus, the total plan area of ineffectually confined core concrete at the level of the hoops when there are n longitudinal bars is

$$A_i = \sum_1^n \frac{\left(w_i^{'}\right)^2}{6}. \tag{11}$$

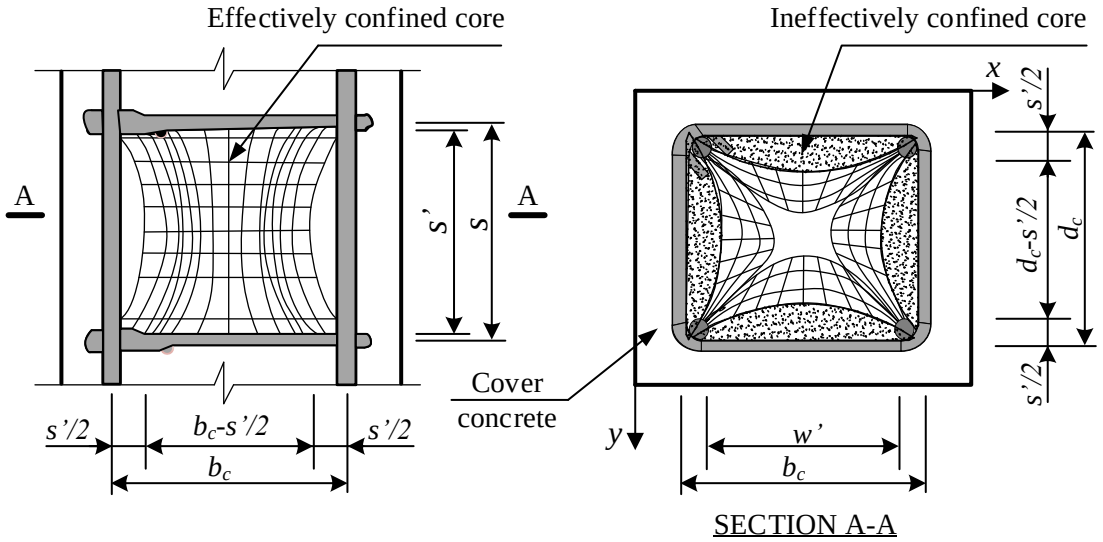

Figure 3. Effectively confined core for rectangular hoop reinforcement

Incorporating the influence of the ineffective areas in the elevation (Figure 3), the area of effectively confined concrete core at midway between the levels of transverse hoop reinforcement is determined as

$$A_e = \left(b_c d_c - \sum_1^n \frac{\left(w_i'\right)^2}{6} \right) \left(1 - \frac{s'}{2b_c}\right) \left(1 - \frac{s'}{2d_c}\right), \tag{12}$$

where b_c and d_c are the core dimensions to centerlines of perimeter hoop in x and y directions, respectively, where $b_c > d_c$. Also, the area of concrete core enclosed by the perimeter hoops is given by Eq. (10). Hence from Eq. (9) becomes

$$k_e = \left(1 - \sum_1^n \frac{\left(w_i'\right)^2}{6 b_c d_c} \right) \left(1 - \frac{s'}{2b_c}\right) \left(1 - \frac{s'}{2d_c}\right) \Big/ \left(1 - \rho_{cc}\right). \tag{13}$$

It is possible for rectangular reinforced concrete members to have different quantities of transverse confining steel in the x and y directions. These may be expressed as:

$$\rho_x = \frac{A_{sx}}{s d_c};\ \rho_y = \frac{A_{sy}}{s d_c}, \tag{14}$$

where A_{sx} and A_{sy} are the total area of transverse bars running in the x and y directions, respectively.

The lateral confining stress on the concrete (total transverse bar force divided by vertical area of confined concrete) is given in the x, y direction as

$$f_{lx} = \frac{A_{sx}}{sd_c} f_{yh} = \rho_x f_{yh};\ \ f_{ly} = \frac{A_{sy}}{sd_c} f_{yh} = \rho_y f_{yh}. \tag{15}$$

From Eq. (8), the effective lateral confining stresses in the *x* and *y* directions are

$$f_{lx}^{'} = k_e \rho_x f_{yh};\ \ f_{ly}^{'} = k_e \rho_y f_{yh}. \tag{16}$$

Scott et al. [10] proposed the formula to determine maximum available core concrete compressive strain ε_{cu} in stress-strain in Figure 2 as:

$$\varepsilon_{cu}^{x} = 0.004 + 0.9\rho_x f_{yh} / 300; \varepsilon_{cu}^{y} = 0.004 + 0.9\rho_y f_{yh} / 300. \tag{17}$$

In Eq. (17), it is assumed that the maximum of ε_{cu} for unconfined concrete is 0.004 [5, 10].

2.3. Model, equation of motion and solution

In order to model the frame structure of the building with confined concrete, the columns are assigned fiber-section elements. Accordingly, the cross-section of fiber elements is distinguished into two parts: unconfined concrete (cover concrete part) and confined concrete (core concrete - limited by reinforcements), as shown in Figure 4. The reinforced concrete slab and wall are modeled by shell elements with unconfined concrete. The structural model is then created by using OpenSees Navigator.

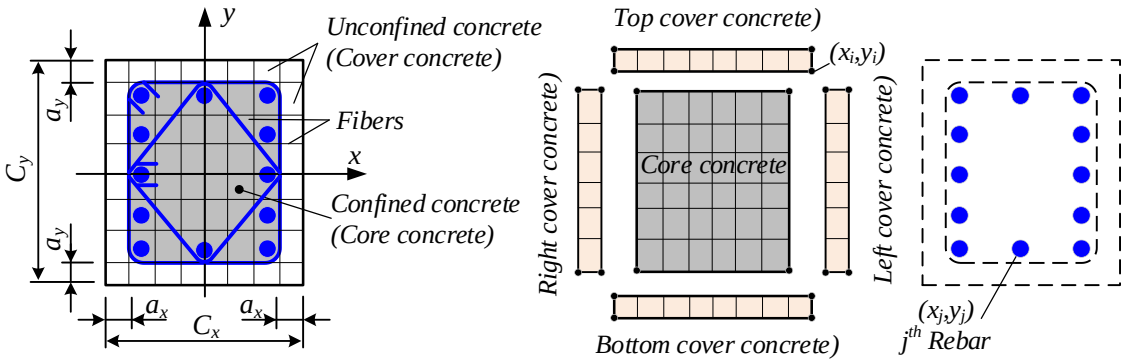

Figure 4. Fibre section model.

The equation of motions for the nonlinear model subjected to earthquake is expressed as [16]:

$$[M]\{\ddot{U}\} + [C]\{\dot{U}\} + f_S(\{U\}) = \{P(t)\}, \tag{18}$$

where $f_S(\{U\})$ is the resisting force, calculated as function of displacement vecto $\{U\}$; $[M], [C]$ are the mass and damping matrices of structure, respectively; $\{P(t)\}$ is the earthquake loading vector defined by:

$$\{P(t)\} = -[M]\{I\}\ddot{u}_g, \tag{19}$$

with $\{I\}$ is a unit vector giving the direction of load application; $\ddot{u}_g$ is a ground acceleration.

The Rayleigh damping matrix $[C]$ is specified as a combination of stiffness and mass-proportional damping matrices with damping ratio $\zeta_1 = \zeta_2 = 0.05$ [15, 16].

Since the material's behavior is considered nonlinear, the Eq. (18) therefore is nonlinear-equation. The combination of Newmark integration method and Newton-Raphson iteration [16] is adopted solve this equation.

The convergence test is applied to the following equation: norm displacement increment [15, 21]:

$$\sqrt{\{\Delta U\}^T \{\Delta U\}} \le Tolerance. \tag{20}$$

Based on the above algorithm, the authors developed appropriate code for considered Mander's model that is integrated into OpenSees' source code to determine model parameters for "*concrete01 model"* in analysis.

3. Numerical analysis

3.1. Description of the building structure

In this section, a set of numerical analysis for a building structure is performed. A typical model 3D of a multi-story building is considered with the detailed properties of the structure as below:

- The reinforced concrete building has 10 floors, including a basement and 09 stories. The floor height is 4.2 m. The plan has five bays in the X and three bays in the Y direction, as shown in Figure 5a.

- Structural component includes: The cross-section of main beam systems is 30 cm x 60 cm, sub-beam is 30 cm x 50 cm. The cross-section dimensions of columns: from 1st to 3rd story is 70 cm x 70 cm; from 4th to 7th story is 60 cm x 60 cm; from 8th to the roof is 50 cm x 50 cm. The concrete wall thickness is 25 cm; the floor thickness is 15 cm.

- Grade of structural concrete: B25; grade of longitudinal reinforcement: CB 300-V and transversal reinforcement: CB 240-T (TCVN 5574:2018) [2].

- Load acting: The floor loading: dead load 200 daN/m^2, live load 240 daN/m^2 and the roof loading: dead load 200 daN/m^2, live load 100 daN/m^2.

The building structure is modeled and investigated by OpenSees software. In the framework of this analysis, the column structures are modeled by fiber-section elements, the longitudinal reinforcements are assigned rebar elements, as shown in

Figure 4. According to the OpenSees model, for the fiber elements, the behavior of concrete parts is represented by Mander's model with "*concrete01"* model and *"steel01"* model representing bilinear model, is applied for reinforcement's behavior. The beam structures are modeled using 3D beam-column elements. The reinforced concrete slabs and walls are modeled using shell elements with linear elastic properties.

Stress-strain points for the considered column's section are illustrated in Figure 7. For each beam and column element, 5 typical cross-sections are specified for integral calculation.

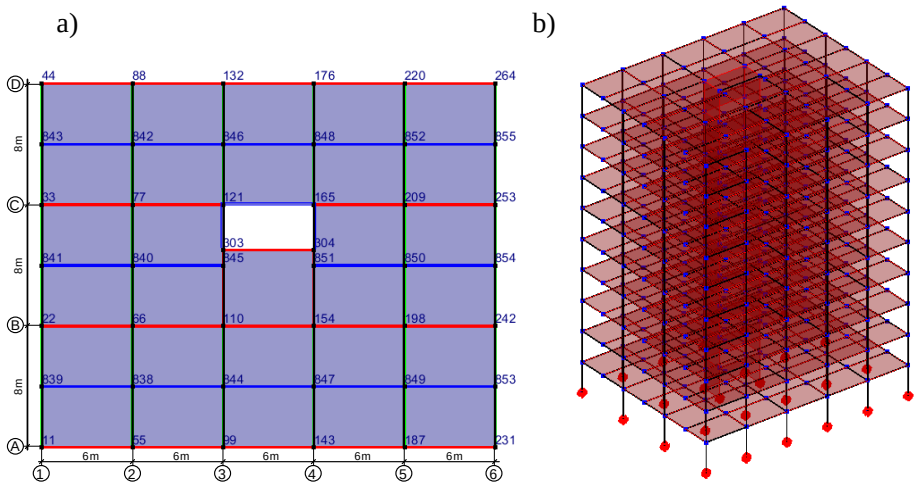

Figure 5. (a) Specific floor plan model and (b) 3D model.

The designed building supports on the soil class B, located in the region of Son La, Viet Nam with the design spectral acceleration according to TCVN 9386:2012, representative by a_{gR} = 0.1893g [22]. In this study, Northridge earthquake record is selected, transformed, and scaled, by using SeismoMatch, to match the target spectrum determined by TCVN 9386-2012 with 5% damping as given in Figure 6.

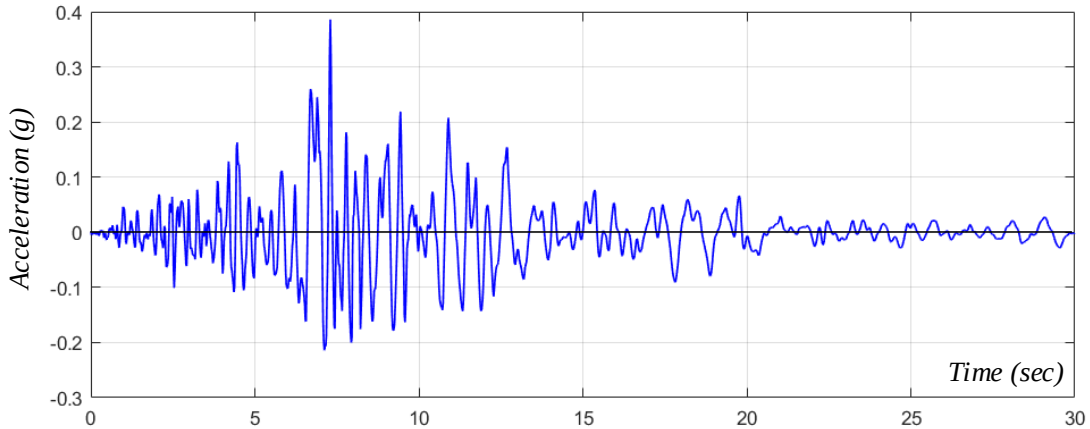

Figure 6. Ground motion time history (Northridge earthquake transformed and scaled).

3.2. Calculated the parameters of the stress-strain model

- For unconfined concrete for cover concrete: E_b = 30 GPa; f'_{c0} = 18.5 MPa; f'_{cu} = 9.25 MPa; $\varepsilon_{c0} = 0.002$ and $\varepsilon_{cu} = 0.0035$ [2].

- For confined concrete for core concrete: E_b = 30 GPa. Based on Mander's model, the parameters are calculated and presented in Table 1.

- The parameters of the steel stress-strain model based on bilinear model, where E = 200 GPa; f_y = 300 MPa, harding ratio, b = 0.02.

Table 1. The parameters of the Mander's stress-strain model

Specimen	Longgitudinal Steel		Transverse Steel		Confined concrete			
	Number and size (mm)	ρ (%)	Size and spacing (mm)	ρ_t (%)	f'_{cc} (MPa)	f'_{cu} (MPa)	ε_{cc}	ε_{cu}
C70x70	16D22	1.70	4D10a150	0.35	22.71	18.45	0.0043	0.0162
C60x60	16D20	2.02	4D10a150	0.42	23.26	18.81	0.0046	0.0186
C50x50	16D18	2.57	4D10a150	0.53	23.93	19.09	0.0049	0.0225

3.3. Results and discussions

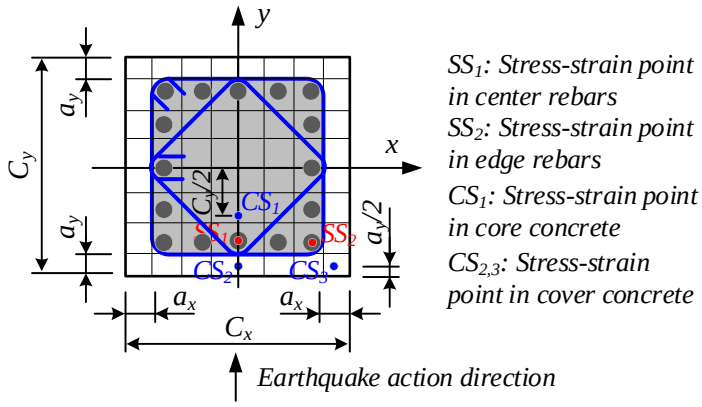

Figure 7. Stress-strain points for section in OpenSees.

Seismic time-history responses of the base shear force and the lateral displacement at the top floor are shown in Figure 8, including also a comparison of the analysis results between the Etabs software (linear elastic behavior) and OpenSees software (nonlinear behavior). The obtained results present a good accordance between the two methods. When compared with the linear elastic model, the nonlinear model results in a higher maximum displacement (12.29%) but a lower maximum base shear force (6.53%) as in Table 2. Logically, this observation is highly consistent with mechanical principles as nonlinear behavior of materials has a certain effect on the seismic response of structures. These reasonable results suggest that it is appropriate to use OpenSees software for nonlinear seismic analysis of buidings.

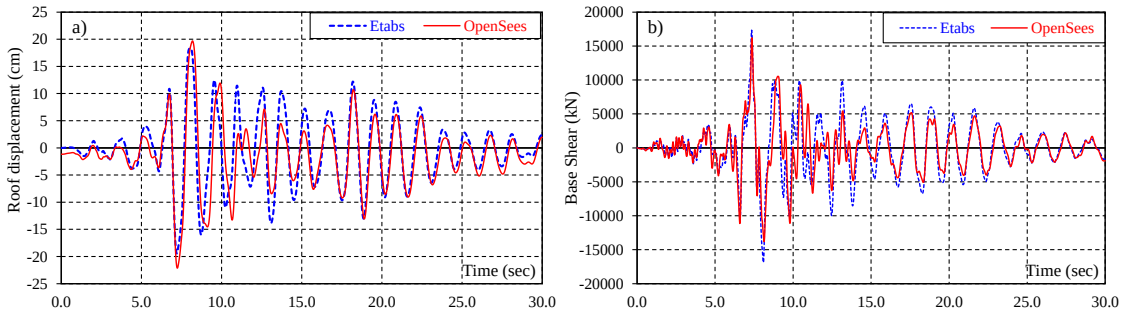

Figure 8. Time history responses of base shear forces (a) and lateral displacements at the top story (b).

Table 2. The parameters of the Mander's stress-strain model

Value	Roof Displacement (cm)			Base shear (kN)		
	Etabs	OpenSees	Compare (%)	Etabs	OpenSees	Compare (%)
Max	18.365	19.700	-6.776	17.350	16.217	6.529
Min	-19.416	-22.137	-12.290	-16.868	-13.804	18.164

Figure 9 shows the stress-strain relationship in rebar for the two considered points of SS1 and SS2 (see Figure 7). Namely, Figure 9a presents the maximum responses of stress and strain of rebars for column C91, (the first story, axes B-3); Similarly, Figure 9b shows the results for column C83 (the third story, axes A-3).

As an observation, when the maximum stress is greater than the yield stress of the considered material, F_y = 300 MPa ($\sigma_{\max}^{SS1/C91}$ = 302.8 MPa, $\sigma_{\max}^{SS2/C91}$ = 316.4 MPa), the behavior of rebars becomes nonlinear. For column 83 (see Figure 9b), the rebars present a linear behavior and the maximum stress response is always lower than the yield stress of material ($\sigma_{\max}^{SS1/C83}$ = 108.3 MPa, $\sigma_{\max}^{SS2/C83}$ = 163.8 MPa).

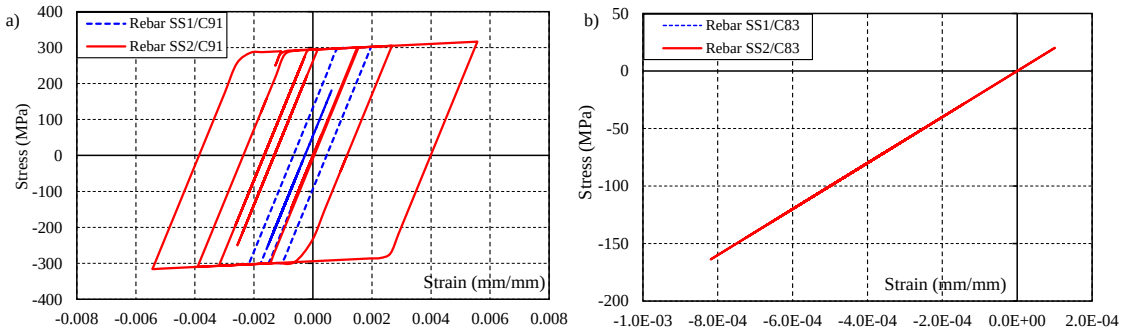

Figure 9. Comparison of stress-strain relationship in rebar between SS1 and SS2 point: a) Column 91/B-3 axis/ 1st story and b) Column 83/A-3 axis/ 3rd story.

Figure 10 presents the stress-strain relationship in the concrete part for three considered points of CS1, CS2, and CS3 (see Figure 7), where CS1 is representative of

the points located in confined concrete areas and CS2, CS3 are the points located in the unconfined concrete areas. More specifically, the maximum responses of stress and strain of concrete are presented in Figure 10a) for column C91 (the first story, axes B-3) and Figure 10b) for column C83 (the third story, axes A-3).

Based on the obtained results in Figure 10 and Table 3, it is found that for confined concrete areas (point CS1), the maximum stress and strain is lower than the yield strength, the material behavior therefore is still in the elastic phase.

On the other hand, for unconfined concrete areas (points CS2, CS3), the maximum response of stress and strain is beyond the elastic limit of materials. The observed material behavior, therefore, is nonlinear (see Figure 10). This obtained result suggests that the confined concrete provided a larger elastic limit when compared to the unconfined concrete.

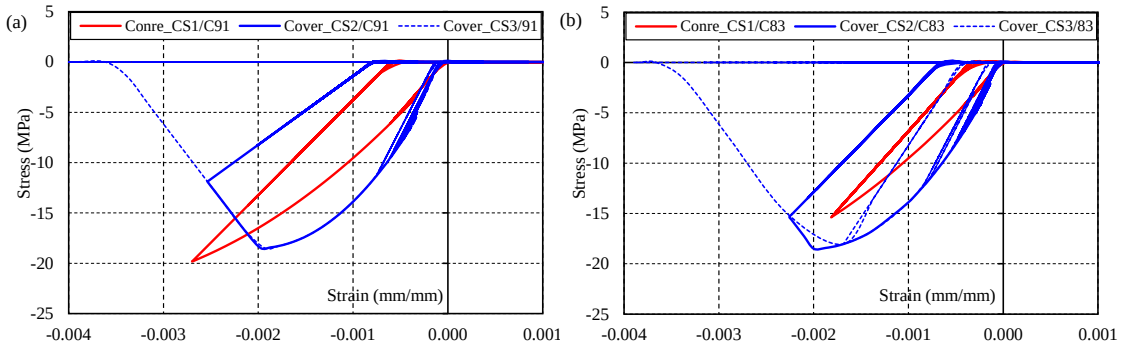

Figure 10. Comparison of stress-strain relationship in concrete between CS1, CS2 and CS3 point: a) Column 91/B-3 axes/ 1st story and b) Column 83/A-3 axes/ 3rd story.

Table 3. Comparisons of max value between model and analyzed results

		1st story/B-3 axis/C91/Point			3rd story/ B-3 axis C83/Point		
		CS1	CS2	CS3	CS1	CS2	CS3
Model	f'_{c0} (f'_{cc}) (MPa)	25.11	18.50	18.50	26.01	18.50	18.50
	ε_{c0} (ε_{cc})	0.0056	0.0020	0.0020	0.0061	0.0020	0.0020
Analysis	σ_{max} (MPa)	19.816	18.500	18.483	15.390	18.500	18.059
	Strain	0.0027	0.0020	0.0019	0.0018	0.0020	0.0017

4. Conclusions

The paper presents the seismic analysis method of a multi-story building using the fiber column elements with effects of confined concrete part, conducted by OpenSees software. For this study, Mander's nonlinear model is employed to model the confined concrete's behavior and bilinear model represents the reinforcement behavior. The obtained results showed that Mander's model was appropriate for the nonlinear modeling of the

reinforced concrete frame structures. By using this model, the structure ductility significantly increases. In addition, it also allows determining in detail the stress-strain state of structures, which is highly effective for evaluating the bearing capacity and the energy dissipation capacity of structures subjected to earthquakes as specified in design codes.

References

[1] EN 1992-1-1, Eurocode 2: Design of concrete structures, part 1-1: General rules and rules for buildings, 2004.

[2] TCVN 5574: 2018 Tiêu chuẩn thiết kế kết cấu bê tông cốt thép.

[3] CSI 2018 Etabs V17.0.1

[4] Code M 1990 CEB-FIP Model Code 462

[5] Mander J B, M.J.N P and Park R "Theoretical stress-strain model for confined concrete", *Journal of Structural Engineering*, 114, 1804-26, 1989.

[6] Chung H, Yang K, Lee Y and Eun H, "Stress - strain curve of laterally confined concrete", 24, 1153-63, 2002.

[7] Sheikh B S A and Uzumeri S M, "Analytical model for concrete confinement in tied columns", *Journal of the Structural Division*, 108, 2703-22, 1983.

[8] Sheikh S A and Uzumeri S M, "Strength and ductility of tied concrete columns", *Journal of the Structural Division*, 106, 1079-102, 1980.

[9] Kent D C and Park R, "Flexural Members with Confined Concrete", *Journal of the Structural Division*, 97, 1969-90, 1971.

[10] Scott B D, Park R and Priestley M J N, "Stress-Strain Behavior of Concrete Confined by Overlapping Hoops at Low and High Strain Rates", *ACI Journal*, 13-27, 1982.

[11] Mander J B, Priestley M J N and Park R, "Onserved Stress-Strain Behavior of Confined Concrete", *Journal of Structural Engineering*, 114, 1827-49, 1989.

[12] Legeron F and Paultre P, "Uniaxial Confinement Model for Normal- and High-Strength Concrete Columns", *Journal of Structural Engineering*, 129, 241-52, 2003.

[13] Paultre P and Légeron F, "Confinement Reinforcement Design for Reinforced Concrete Columns", *Journal of Structural Engineering*, 134, 738-49, 2008.

[14] Pinho R, "Nonlinear Dynamic Analysis of Structures Subjected to Seismic Action", *Advanced Earthquake Engineering Analysis*, p. 218, 2007.

[15] Clough; R W and Penzien J, "Dynamics of structures", *Berkeley: Computers & Structures, Inc.*, 2010.

[16] Cheng F Y, "Matrix Analysis of Structural Dynamics", *Marcel Dekker, Inc.*, 2017.

[17] Ziemian R D, "Examples of frame studies used to verify advanced methods of inelastic analysis", Plastic hinge based methods for advanced analysis and design of steel frames, 1993.

[18] OpenSees https://opensees.berkeley.edu/wiki/index.php/OpenSees-User

[19] Melo J, Fernandes C, Varum H, Rodrigues H, Costa A and Arêde A, "Numerical modelling of the cyclic behaviour of RC elements built with plain reinforcing bars", *Engineering Structures,* 33, 273-86, 2011.

[20] Trần Ngọc Cường, "Áp dụng phương pháp phân tích động phi tuyến theo lịch sử thời gian mới vào phần mềm OpenSees", *Kết cấu và Công nghệ xây dựng*, 1, 17-26, 2017.

[21] Mazzoni S, Mckenna F, Scott M H and Fenves G L, "OpenSees Command Language Manual", 2007.

[22] TCVN 9386, Thiết kế công trình chịu động đất, Phần 1, 2012.

ỨNG XỬ ĐỘNG ĐẤT CỦA KẾT CẤU NHÀ NHIỀU TẦNG BÊ TÔNG CỐT THÉP VỚI BÊ TÔNG BỊ HẠN CHẾ

Nguyễn Văn Tú, Nguyễn Xuân Đại, Lê Quốc Kỳ

Tóm tắt: *Bài báo trình bày phương pháp phân tích động đất của nhà nhiều tầng bằng bê tông cốt thép sử dụng mô hình phi tuyến của Mander cho ứng xử của bê tông bị hạn chế và mô hình song tuyến tính cho ứng xử của cốt thép. Tác động của động đất lên công trình được phân tích theo phương pháp phân tích lịch sử thời gian. Kết cấu công trình được mô hình hóa bằng phương pháp phần tử hữu hạn dựa trên phần mềm OpenSees. Các phản ứng nhận được của nội lực, chuyển vị, ứng suất biến dạng phù hợp với mô hình nghiên cứu và có thể ứng dụng trong phân tích kết cấu nhà nhiều tầng bê tông cốt thép chịu động đất.*

Từ khóa: Bê tông bị hạn chế; bê tông không bị hạn chế; mô hình ứng suất - biến dạng của bê tông bị hạn chế; lõi bê tông; phân tích phi tuyến hệ khung bê tông cốt thép; lớp bê tông bảo vệ.

Received: 16/10/2021; *Revised:* 26/11/2021; *Accepted for publication:* 28/12/2021

❑